Developmental Cell
Article

Specific GATA Factors Act as Conserved Inducers of an Endodermal-EMT

Kyra Campbell,[1,2] Gavin Whissell,[2] Xavier Franch-Marro,[3] Eduard Batlle,[2,4] and Jordi Casanova[1,2,5,*]
[1]Institut de Biologia Molecular de Barcelona-CSIC
[2]Institut de Recerca Biomèdica de Barcelona
Parc Cientific de Barcelona, 08028 Barcelona, Spain
[3]Institut de Biologia Evolutiva CSIC-UPF, Passeig de la Barceloneta, 37-49, 08003 Barcelona, Spain
[4]Institució Catalana de Recerca i Estudis Avançats (ICREA), Passeig Lluís Companys 23, 08010 Barcelona, Spain
[5]I dedicate this paper to the memory of my father, Damià Casanova, who, I have recently been told, once guessed I would work in this field
*Correspondence: jcrbmc@ibmb.csic.es
DOI 10.1016/j.devcel.2011.10.005

SUMMARY

The epithelial-to-mesenchymal transition (EMT) converts cells from static epithelial to migratory mesenchymal states (Hay, 1995). Here, we demonstrate that EMT in the *Drosophila* endoderm is dependent on the GATA-factor Serpent (Srp), and that Srp acts as a potent trigger for this transition when activated ectopically. We show that Srp affects endodermal-EMT through a downregulation of junctional dE-Cadherin (dE-Cad) protein, without a block in its transcription. Moreover, the relocalization of dE-Cad is achieved through the direct repression of *crumbs (crb)* by Srp. Finally, we show that hGATA-6, an ortholog of Srp, induces a similar transition in mammalian cells. Similar to Srp, hGATA-6 acts through the downregulation of junctional E-Cad, without blocking its transcription, and induces the repression of a Crumbs ortholog, *crb2*. Together, these results identify a set of GATA factors as a conserved alternative trigger to repress epithelial characteristics and confer migratory capabilities on epithelial cells in development and pathogenesis.

INTRODUCTION

The epithelial-to-mesenchymal transition (EMT) plays crucial roles during development, and when activated inappropriately can promote tumor progression and metastasis. This process converts cells from static epithelial to migratory mesenchymal states (Hay, 1995; Thiery et al., 2009) and is often carried out to different extents, as many cells adopt mesenchymal behaviors yet retain some epithelial features (Revenu and Gilmour, 2009). One of the best-known examples of an EMT underlies the formation of the *Drosophila* mesoderm, which is triggered by Snail (Sna). Subsequent to its discovery in *Drosophila*, genes of the *sna* family were found to induce EMT during the development of many organisms and inappropriately activated in several forms of cancer. A similar transition occurs during the formation of the *Drosophila* endoderm, when epithelial cells convert to a migratory mass of mesenchymal cells (Campos-Ortega and Hartenstein ,1985; Skaer, 1993; Reuter, 1994; Tepass and Hartenstein, 1994a), which migrate through the embryo and later re-epithelialize to give rise to a large portion of the intestinal tract. However, in contrast to the mesoderm, this transition seems to occur independently of Sna (Reuter and Leptin, 1994; Tepass and Hartenstein, 1994a).

Formation of the *Drosophila* intestinal tract originates from two groups of cells at each pole of the blastoderm. In particular, cells from the posterior region give rise to the hindgut, of ectodermal origin, and the posterior midgut (PMG), of endodermal origin (Campos-Ortega and Hartenstein, 1985). While derived from a common primordium, hindgut and PMG cells undergo dramatically different cell behaviors during development. Hindgut cells remain epithelial and relatively static throughout, whereas PMG cells temporarily adopt mesenchymal behavior and initiate migration toward the center of the embryo, where they fuse with the anterior midgut (AMG) to form a continuous intestinal tract (Reuter et al., 1993; Campos-Ortega and Hartenstein, 1985; see Movie S1 available online). The decision of whether to form hindgut or the PMG is regulated by the activity of a single gene product, the GATA factor Serpent (Srp), which is active in the cells giving rise to the PMG. In *srp* mutants a homeotic transformation has been reported, as an ectopic hindgut forms at the expense of the PMG (Reuter, 1994).

Here, we investigate the role of Srp during endoderm development and show that Srp is both necessary and sufficient to induce epithelial cells to undergo a transition to a non-apicobasally polarized, motile state. At the molecular level, this transition involves the repression of genes encoding the apically localized proteins Crumbs (Crb), Stardust (Sdt), and Stranded-at-second (SAS). In contrast, while adherens junction-associated proteins are delocalized, they are not transcriptionally repressed. We show that rather than abolishing *dE-Cadherin (dE-Cad)* gene transcription, Srp acts at the level of dE-Cad protein and regulates its membrane localization. Moreover, this relocalization of dE-Cad requires the direct repression of *crumbs (crb)* by Srp. We extend these results by showing that human GATA4 and GATA6 can also induce an epithelial to nonpolarized migratory cell transition, and similarly this occurs in an E-Cadherin (E-Cad) transcription independent manner. Furthermore, overexpression of GATA6 induces the transcriptional repression of a Crumbs ortholog, *crb2*. These results unveil the role of

specific GATA factors as inducers of an EMT that is characterized by affecting E-Cad protein localization rather than transcription.

RESULTS

PMG Cells Undergo an Epithelial Transition Characterized by a Loss of Apico-Basal Polarity and Downregulation of Junctional dE-Cad

To better understand the endoderm transition, we analyzed markers for cell polarity, adhesion, and the cytoskeleton prior to, and during PMG migration. Analysis of F-actin (F-Act) and apico-basal markers reveals that in stage 9 embryos, endoderm cells are fully polarized epithelial cells (Figures 1A, 1D, 1G, 1J, and 1M). Electron microscopy studies showed that posterior endoderm cells possess complete zonula adherens during stages 6–9 (Tepass and Hartenstein, 1994b); accordingly, we find a tight apical localization of dE-Cad in endoderm cells throughout these stages (Figure 1P and data not shown). During stage 10, a loss of epithelial characteristics is first apparent in cells at the most distal region of the PMG, and later throughout the PMG. Cells lose their columnar appearance, become more rounded and irregular in shape (Figures 1B, 1C, 1N, and 1O). Apical and junctional proteins are gradually lost from the cell surface, and the overall levels of these proteins dramatically decrease (Figures 1F, 1I, 1L, and 1R). When PMG cells initiate migration, apical and subapical proteins Stranded-at-second (SAS), Crumbs (Crb), and Stardust (Sdt) are no longer detectable, while low levels of junctional dE-Cad, Bazooka (Baz), and atypical protein kinase C (aPKC) remain (Figures 1F, 1I, 1L, and 1R; Figure S1). Indeed dE-Cad, Baz, and aPKC lose their tight apical localization and instead colocalize to dynamic punctate accumulations at the cell membrane (Figure S1; Movie S2). Electron microscopy studies previously showed that after adherens junctions fragment in the endoderm, low levels of spot adhesion junctions are present throughout the PMG (Tepass and Hartenstein, 1994b). We suggest that dE-Cad/Baz/aPKC could localize to spot adhesion junctions, which may act as dynamic adhesions facilitating cohesive migration of the mesenchymal cell mass.

Srp Activity Is Required for Endodermal-EMT in the PMG

Formation of the PMG depends on *srp* (Reuter, 1994) and occurs independently of *sna* genes (Reuter and Leptin, 1994; Tepass and Hartenstein, 1994a) (Figure S2), conversely to AMG formation that requires both *srp* and *sna* (Reuter and Leptin, 1994). Thus, to analyze the role of Srp in endoderm transition, we have focused our analysis on the PMG. In *srp* mutants, endodermal cells retain epithelial shape and polarity (Figures 2A and 2B) and dE-Cad remains tightly localized to the apical domain (Figure 2B). Thus, the endodermal-EMT depends on Srp activity.

Maintenance of Srp Activity Prevents PMG Cells from Reforming an Epithelium

Next, we looked to see when Srp protein is expressed in the PMG, and found that it is first expressed during stage 5 (data not shown), indicating that there is a time lag of 2 hr before endodermal EMT becomes visible at the morphological level. This suggests that a certain threshold of Srp may need to be reached for it to become active, or that its activity is being repressed by an unknown mechanism during stages 5–9. At the stage when we see a downregulation of Crb and Sdt, and delocalization of junctional proteins, Srp is expressed very strongly in the PMG (Figure 2C, arrows); however, during stages 11 and 12, there is a gradual loss of Srp expression in the PMG (Figures 2D and 2E, arrows). As Srp starts to disappear from the cells as they start migrating, we reasoned that the temporally restricted expression

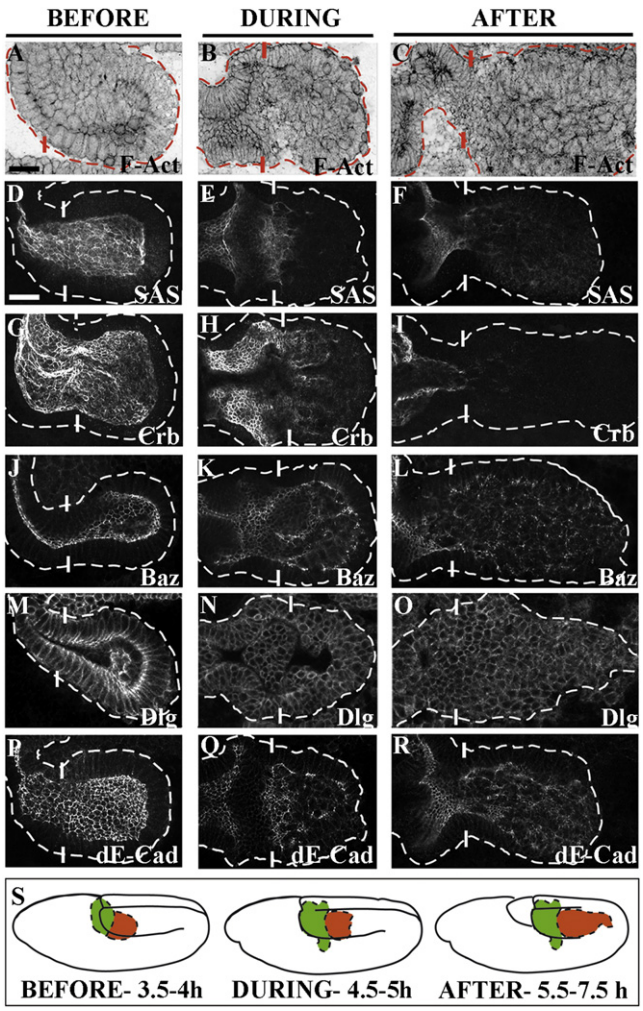

Figure 1. As Endodermal Cells Undergo EMT They Lose Epithelial Morphology and Apico-Basal Polarity and Downregulate Junctional dE-Cad

(A–R) Wild-type embryos stained for the cytoskeletal marker F-act (A-C), the apical proteins SAS (D–F), Crb (G–I), or Baz (J–L), the basolateral marker Dlg (M–O), or the adherens junction marker dE-Cad (P–R). Before is 3.5–4 hr after fertilization (stage 9), during is 4.5–5 hr (stage 10), and after is 5.5–7.5 hr (stage 11 to early stage 12). The PMG is outlined by dotted lines; vertical lines demark the separation between the hindgut and PMG during stage 9, first column, and between the Malpighian tubules and PMG during stages 10 and 11, second and third columns. The PMG is always to the right of the vertical lines. Scale bars, 20 μm.

(S) Schematic showing the position of the PMG (red) with respect to the hindgut/Malpighian tubule primordium (green) and the rest of the embryo during stages 9–12.

See also Figure S1 and Movies S1 and S2.

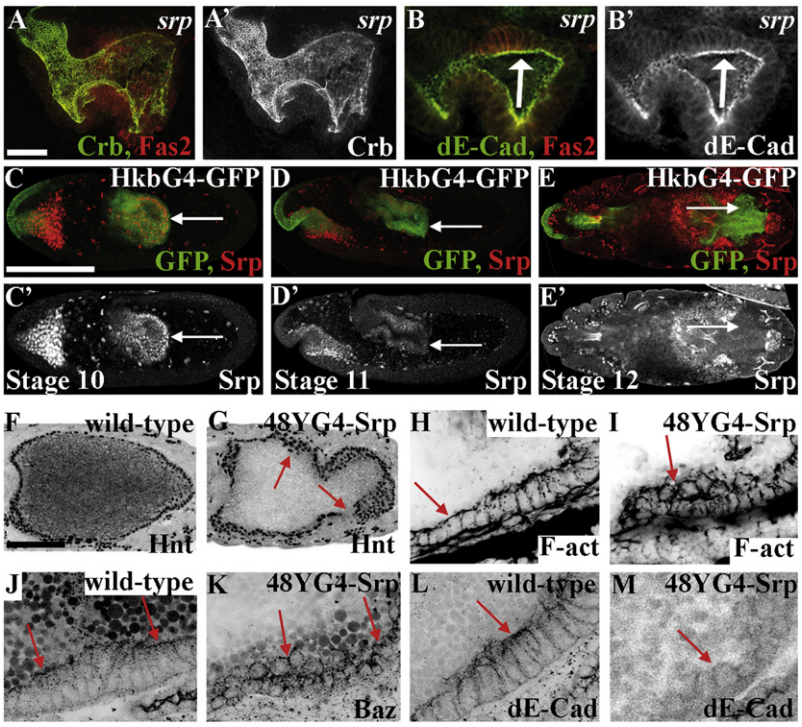

Figure 2. Srp Is Required for PMG EMT and Maintenance of Srp Expression Prevents PMG Cells from Redeveloping Epithelial Characteristics

(A and B) Stage 12 *srp* mutants stained for the basolateral marker Fascicilin2 (Fas2), and Crb (A) or dE-Cad (B). In *srp* mutants, PMG cells remain columnar in shape (B, arrow) and tightly localize both Crb and dE-Cad to their apical domains.

(C–E) Srp expression during stages 10 (C), 11 (D), and 12 (E); arrows point to the PMG. Srp expression is lost from PMG cells during stages 11–12 (D and E).

(F–M) Stage 15 wild-type (F, H, J, and L) and sustained expression of Srp (G, I, K, and M) in the endoderm using 48Y-Gal4. (F and G) Srp overexpression leads to a discontinuous midgut epithelium, containing breaks and cell multilayering (compare F with G, arrows). Both F-act and Baz are found delocalized around the cell cortex (I and K, arrows), and dE-Cad is almost undetectable in the cells (M, arrow). Black and white fluorescence images were color-inverted in Photoshop.

Scale bars: (A) and (B), 20 μm; (C)–(E), 100 μm; (F) and (G), 50 μm; (H)–(M), 20 μm. See also Figure S2.

of Srp could be related to the fact that PMG cells only undergo a transient transition to mesenchymal behavior; once endodermal cells have migrated to their final position, they undergo a reverse transition, mesenchymal-to-epithelial, forming the midgut epithelium (Figures 2F, 2H, 2J, and 2L) (Tepass and Hartenstein, 1994a). To test this, we provided sustained Srp expression at the time when it would normally be turned off (see Experimental Procedures). Under these circumstances, the midgut epithelium does not properly form, and we detect multicell layered stretches instead of a normal monolayered epithelial morphology (Figures 2G and 2I). Analysis of several markers reveals that continued expression of Srp prevents PMG cells from reestablishing epithelial characteristics (Figures 2H–2M). Notably, under these conditions dE-Cad was almost undetectable in PMG cells (Figure 2M). Altogether, these results indicate that *srp* has to be turned off for endodermal cells to regain epithelial characteristics.

Ectopic Expression of Srp Induces a Similar EMT in Epithelial Cells

To further explore the ability of Srp to promote such transitions, *srp* was ectopically expressed in stripes of cells in the embryonic epidermis, which remains epithelial throughout development. Upon *srp* overexpression, cells appear disorganized and dispersed, with stripes broken and fusing across compartment boundaries (Figure 3B; Figure S3B). Furthermore, the cells are no longer present as a monolayer at the cell surface, and instead form multilayered clusters projecting into the embryo (Figures 3D–3F, arrows). Cells lose their columnar morphology and become more elongated and irregular in shape (Figures 3D–3F). Internalized epidermal cells localize F-Act throughout the cell cortex and do not express Crb, and dE-Cad becomes relocalized around the cell (Figures 3E and 3F; Figures S3D and S3E). In some internalized cells dE-Cad expression is below detectable levels (Figure 3E, arrow). While it could be that dE-Cad is harder to detect in these cells because of its delocalization, it suggests that very high levels of *srp* may induce a downregulation/degradation of dE-Cad protein. Interestingly, the few *srp* overexpressing cells that remain at the surface of the embryo express high levels of Crb and dE-Cad at the apical surface, but have undergone apical constriction (Figures 3D, 3F, and 3G), a common feature of developmental EMTs (Shook and Keller, 2003).

Analysis in living embryos shows that *srp* overexpression leads to the activation of migratory behavior, with cells extending many protrusions (Movies S3 and S4) and moving to more distant sites in the embryo (Figures 3I–3L, arrowheads in Figures 3J and 3L indicate long cords/groups of cells mispositioned in the embryo; Movies S5 and S6). Notably, while cells appear more elongated and protrusive, they do not become dispersed but move collectively through the embryo. Furthermore, *srp* overexpression leads to induction of Matrix metalloproteinase 1 (Mmp1) (Figure 3G), which is known to cleave extracellular matrix components, and thus facilitate invasive migratory cell behavior (Srivastava et al., 2007). Ectopic Srp also induces expression of Forkhead (Fkh) (Figure 3H), an ortholog of the vertebrate FoxA transcription factors. *fkh* has previously been reported to act as a survival factor in a number of *Drosophila* systems, including the midgut (Tepass et al., 1994; Myat and Andrew, 2000; Cao et al., 2007), suggesting that similar to vertebrate *sna* (Barrallo-Gimeno and Nieto, 2005), *srp* overexpression may cause cells to become more resistant to apoptosis and cell death. Altogether, these results indicate that *srp* expression in epithelial cells triggers a loss of epithelial characteristics and acquisition of mesenchymal features (Figure 3M).

Srp-Induced Epithelial Transitions Do Not Act through a Repression of dE-Cad Transcription

The transition from epithelial to migratory nonpolarized cell states involves coordinated changes in numerous cell features

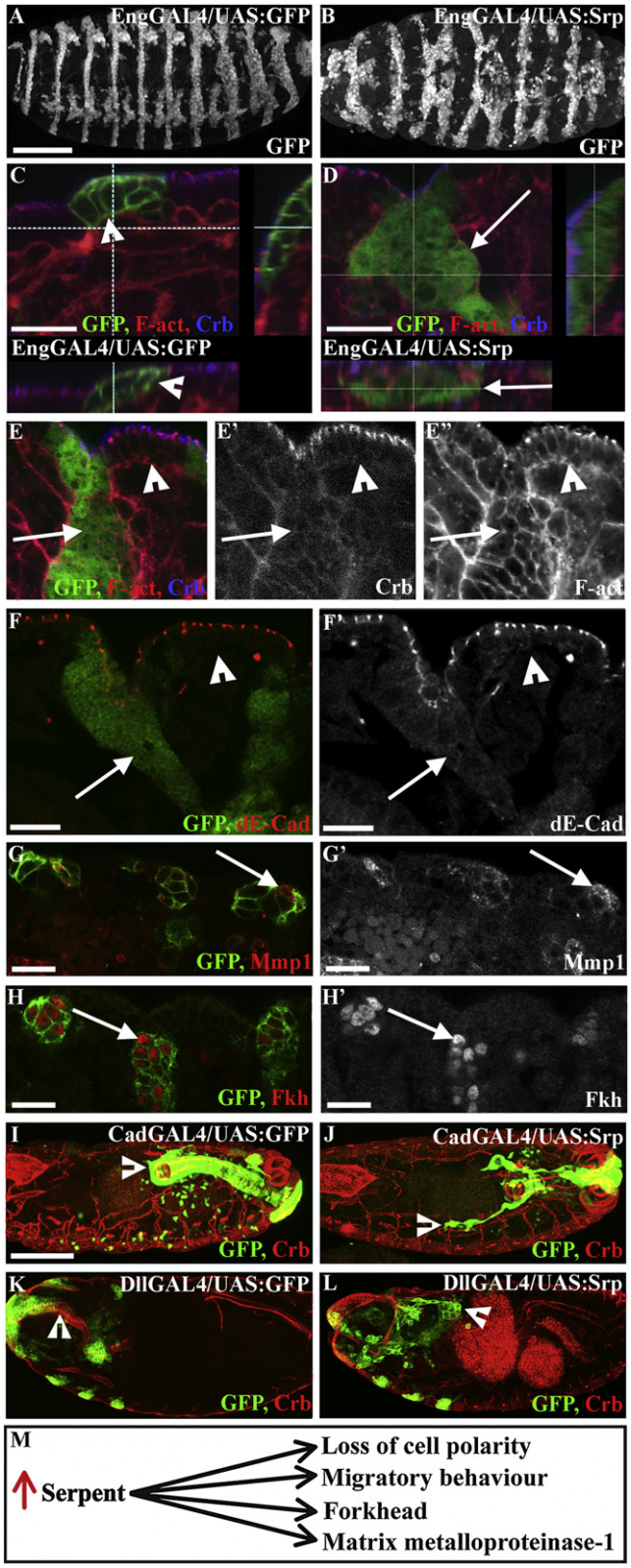

Figure 3. Ectopic Expression of Srp Induces Loss of Epithelial Traits and Acquisition of Migratory and Invasive Behavior

(A–H) Stage 16 embryos expressing either GFP alone under control of EngGal4 (A and C) or both Srp and GFP (B and D–H). Epidermal cells normally form a monolayer at the cell surface (C, E, F, arrowheads). Srp-expressing epidermal cells are found in multilayered clusters that project into the embryo (D–F, arrows, compare with wild-type C). In internalized cells, F-act is found all around the cell cortex (D, arrow), and Crb (D) and dE-Cad (E) are reduced to low levels, or are undetectable (D–F, arrows). Expression of Mmp1 (G) and of Fkh (H) is induced in Srp-positive epidermal cells.

(I–L) Stage 16 embryos expressing either GFP alone (I and K) or both Srp and GFP (J and L) in epithelia in the posterior of the embryo, using Cad-Gal4, which is expressed in the hindgut and anal pads (I and J), or in the anterior, using Dll-Gal4 (K and L). Srp overexpressing epithelia are found at more distant sites in the embryo to in wild-type (compare arrowheads in I and K with J and L). Individual green cells in (I) and (J) are hemocytes, which have phagocytosed GFP-positive apoptotic cells. M, Schematic summarizing the effects of Srp overexpression. EngGal4: Engrailed-Gal4, drives in posterior compartments of the ectoderm; CadGal4: Caudal-Gal4, drives in the posterior of the embryo; DllGal4: Distal-less-Gal4, drives in the anterior of the embryo and some imaginal discs.

Scale bars: (A) and (B), 100 μm; (C–H), 10 μm; (I)–(L), 100 μm.

See also Figure S3 and Movies S3–S6.

such as polarity, shape, adhesion, and migratory and invasive capacities, which in turn are affected by transcription factors such as Sna through the activation and repression of many target genes (reviewed in Barrallo-Gimeno and Nieto, 2005), and this is likely to also be the case for Srp-induced EMT. However, it is clear that while EMT involves many changes in cell behavior, a key step in the initiation of EMT is a functional loss of E-Cad and thus of cell-cell adhesion (Huber et al., 2005; Peinado et al., 2007). Hence, we decided to investigate if Srp effects adhesion through the repression of E-Cad transcription, as has been found for almost all EMT regulators reported to date (Thiery et al., 2009).

During endodermal-EMT dE-Cad loses its apical localization and there is a marked decrease in junctional protein levels (Figures 1P–1R). However, whole-mount in situ hybridization shows that dE-Cad RNA remains expressed in the PMG during endodermal-EMT, and is expressed in migrating PMG cells (Figures 4A–4C). aPKC, which behaves similarly to dE-Cad during PMG-EMT and migration, also shows continued RNA expression (Figures S4A–S4C). Next, we quantified the levels of *dE-Cad* RNA in the PMG at time points before and after endodermal-EMT (see Experimental Procedures) and found that there are no significant variations in *dE-Cad* levels between these two stages (Figure 4D). These data suggest that, in contrast to *sna*, *srp* does not act through the repression of dE-Cad transcription, and this is reinforced by the following three observations. First, sustained expression of *srp* in the midgut does not lead to a loss of dE-Cad RNA, in comparison to *sna* overexpression, which causes dE-Cad RNA to be almost completely absent from midgut cells (Figures 4D–4I). Second, *srp* overexpression does not lead to the induction of known repressors of *dE-Cad* such as *sna* and the ZEB related factors *zfh1* and *zfh2* (Figure S5). Finally, the overexpression of *sna* in the ectoderm does not induce EMT; this is likely due to overexpression of *sna* repressing only the zygotic *dE-Cad* transcription, while the ectoderm is a tissue where the maternal contribution of RNA is sufficient to maintain the tissue throughout embryogenesis (Tepass et al., 1996; Uemura et al., 1996). We conclude that Srp does not induce endodermal-EMT through the repression of *dE-Cad* transcription, rather it triggers a downregulation of junctional dE-Cad protein through the activation/repression of downstream targets.

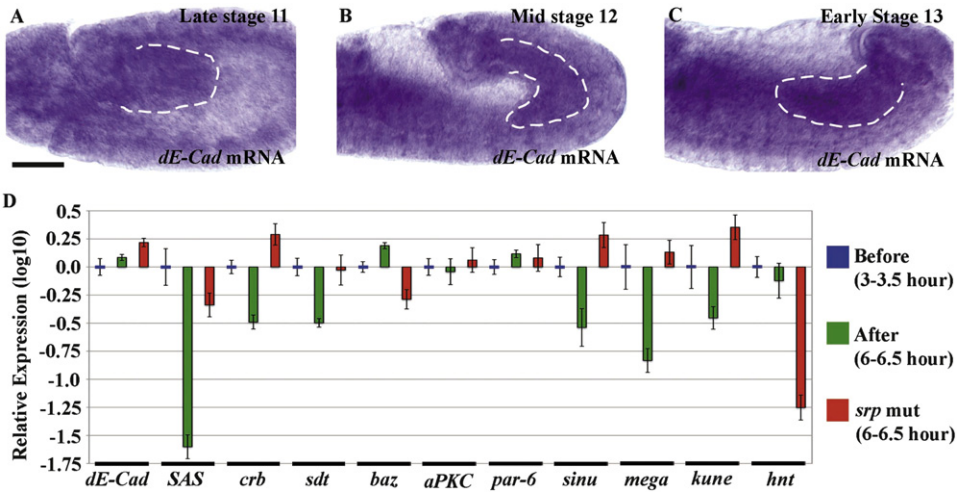

Figure 4. *crb, sdt* and *SAS* Are Transcriptionally Repressed during PMG-EMT, while *dE-Cad* and Components of the Par3 Complex Continue to Be Transcribed

(A–C) In situ hybridization in wild-type embryos for *dE-Cad*. *dE-Cad* remains strongly expressed in the PMG throughout stages 11 (A), 12 (B), and 13 (C).

(D) qRT-PCR analysis of *dE-Cad*, *SAS*, *crb*, *sdt*, *baz*, *aPKC*, *par-6*, *sinu*, *mega*, *kune*, and *hnt* RNA levels in PMGs dissected from 3–3.5 hr (before), 6- to 6.5-hr-old wild-type embryos (After), or from 6–6.5 hr *srp* mutant embryos (*srp* mut). There are no significant changes in the RNA levels of *dE-Cad, baz*, *aPKC*, and *par-6* in the PMG between 3 and 6.5 hr of development, or between wild-type and *srp* mutants. In contrast, *SAS*, *crb*, *sdt*, *sinu*, *mega*, and *kune* become strongly repressed, and this repression is lost in *srp* mutants. *hnt* was used as a control, as it is a known downstream target of Srp, and does not change in expression in the PMG between 3 and 6 hr of development. Gene expression levels were normalized using the endogenous control Actin5C. Error bars indicate SD. Forward and reverse primers are provided in Supplemental Experimental Procedures. See also Figures S4 and S5.

Srp Directly Represses *crb* Transcription

How does Srp induce a loss of cell polarity and adhesion? To address this question, we screened components of the different cell-membrane domains using qPCR to identify genes that were expressed in the PMG prior to endodermal-EMT, but which become repressed in the PMG in a Srp-dependent manner (see Experimental Procedures). We found that genes encoding the apically localized proteins SAS, Crb and Sdt and the basolaterally localized Claudin proteins Sinuous (Sinu), Megatrachea (Mega), and Kune-kune (Kune) become strongly repressed in the PMG during endodermal-EMT, and that this repression is lost in *srp* mutants (Figure 4D). In contrast, we found that there are no significant changes in the levels of the apical Par genes *baz* and *par-6*, or of *aPKC*, during endodermal-EMT, or in *srp* mutants (Figure 4D).

We decided to focus further studies on the key cell polarity regulator Crb, as *crb* is required for the maintenance of epithelial cell polarity and stabilization of adherens junctions (Tepass et al., 1990; Grawe et al., 1996), and in the ectoderm of *crb* mutants dE-Cad is lost from the apical domain and cells lose cell-cell adhesion (Tepass et al., 1990; Grawe et al., 1996), similar to what happens during PMG-EMT. Whole-mount in situs confirmed that *crb* is highly expressed and apically localized in the hindgut and PMG cells prior to stage 10 (Figure 5A) and lost from the PMG during endodermal-EMT, so that its expression is almost undetectable by whole-mount in situ hybridization in late stage 11 and 13 PMG cells (Figures 5B and 5C). In situ hybridization studies in *srp* mutants showed that *crb* RNA levels remain high in PMG cells throughout embryogenesis (Figure 5D), reinforcing the quantitative analysis, and further confirming that *crb* expression is directly or indirectly regulated by Srp.

To further examine the relationship between Srp and *crb,* we performed a ChIP analysis to determine whether Srp is physically associated with *crb* during early stages of development. We focused on a region situated within the first intron of *crb*, termed the *cis*-regulatory module (CRM), as this region has previously been shown to reproduce the endogenous *crb* expression pattern in the mesoderm (Sandmann et al., 2007), and we found that this is also true for the PMG (Figures 5E and 5F). We identified many putative Srp-binding sites within the first intron of *crb,* and tested for Srp binding to these sites by ChIP-PCR analysis. As a positive control for this experiment we found that a putative Srp-binding site in the first intron of *hindsight* (*hnt*), a known target of Srp (Yip et al., 1997), is positive for Srp binding (Figures 5I and 5J). We found that the two sites located within the *crb*-CRM, Crb-2, and Crb-3 show a similar or greater fold change enrichment when compared to hnt and thus are positive for Srp binding (Figures 5I and 5J), pointing to a direct interaction between Srp and *crb* through the *crb*-CRM regulatory region. Conversely, other putative Srp-binding sites outside the CRM were negative for the same assay (Figures 5I and 5J and data not shown) indicating its specificity. To further test if Srp acts through the *crb*-CRM to repress *crb* expression, we next examined the behavior of the *crb*-CRM-lacZ reporter in *srp* mutant and *srp*-overexpressing backgrounds. We found that when Srp is absent, the reporter remains highly expressed in the PMG throughout development (Figure 5G), and conversely, when Srp is overexpressed throughout the embryo, we see that expression of the reporter is almost completely lost (Figure 5H). Taken together these results suggest that Srp directly represses *crb* through binding to GATA sites within the *crb*-CRM region.

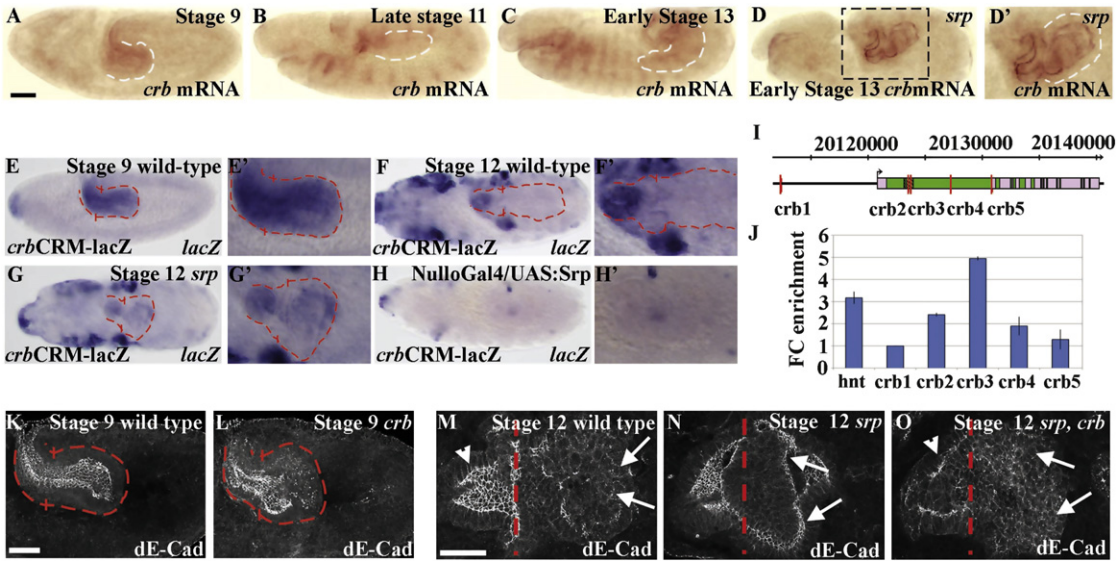

Figure 5. Srp Represses *crb* Transcription

(A–C) In situ hybridization for *crb* in wild-type embryos. *crb* is expressed in the endoderm throughout stage 9 (A) but is not detected in the PMG after it undergoes EMT (B and C).

(D) *crb* is strongly expressed in the PMG in stage 13 *srp* mutants.

(E and F) The *crb*CRM-lacZ reporter reproduces the endogenous crb expression pattern in the PMG (compare E and F with A and C).

(G) In *srp* mutants, the *crb*CRM-lacZ reporter is not repressed in the PMG (compare G with wild-type F).

(H) Overexpression of Srp throughout the embryo, using Nullo-Gal4, causes a general repression of the *crb*CRM-lacZ reporter (compare H with F).

(I) Schematic diagram indicating the location of putative Srp-binding sites (red lines) with respect to the *crb* gene (exons in purple, introns in green), and the location of the *crb*-CRM (shaded in black).

(J) ChIP assays, performed with Srp antibody; data are expressed as fold change enrichment of Srp binding relative to the negative control, and are normalized to input. Forward and reverse primers are provided in Supplemental Experimental Procedures. Error bars indicate SD.

(K and L) In *crb* mutants dE-Cad becomes delocalized in PMG cells during stage 9 (compare L with wild-type K).

(M–O) Stage 12 wild-type (M), *srp* (N) and *srp, crb* double mutant embryos (O) stained for dE-Cad, red lines show the hindgut PMG boundary. (N) In *srp* mutants PMG cells do not undergo EMT and dE-Cad is apically localized throughout the hindgut (arrowhead) and PMG (arrows). (O) In *srp, crb* double mutants, dE-Cad becomes delocalized in PMG cells (arrows in O), similar to in wild-type (arrows in M) and in contrast to in *srp* mutants (arrows in N), while the apical localization of dE-Cad in the hindgut is retained (arrowhead in O). Dotted lines outline the PMG, vertical lines show the hindgut PMG boundary; black box shows the area magnified in (D′).

Scale bars: (A)–(H), 50 μm; (J)–(N), 20 μm.

Loss of Crb Partially Reverts the dE-Cad Phenotype in a Srp Mutant

To investigate the functional relevance of repression of *crb* by Srp we first examined the behavior of dE-Cad in the PMG of *crb* mutants. We found that in *crb* mutants the PMG undergoes a premature delocalization of dE-Cad, with dE-Cad becoming lost from PMG cells as early as stage 9, and a premature alteration of epithelial morphology (Figures 5K and 5L). To provide a functional validation of *crb* repression in the Srp-induced epithelial transition, we generated a double mutant for *srp* and *crb* and found that loss of *crb* partially reverts the dE-cad phenotype and the failure of EMT in the PMG caused by *srp* mutants (Figures 5M–5O, arrows). It should be noted that while dE-Cad becomes delocalized in the PMG of *srp; crb* double mutants, it remains tightly localized in the hindgut (Figure 5O, arrowhead). Together these data indicate that Srp induces a delocalization of dE-Cad through the direct repression of *crb.* Thus, the repression of *crb* by Srp appears to be a central part of the mechanism used to induce endodermal-EMT. However, we have found that ectopic expression of *crb* does not inhibit PMG morphogenesis (data not shown). While this could be due to ectopic Crb not localizing correctly to the apical membrane, it indicates that *crb* downregulation is necessary for endodermal-EMT but *crb* expression is not sufficient to abrogate it. This is in agreement with other genes such as *std* and *SAS* being repressed by Srp in the PMG. Furthermore, it is similar to results for Sna-induced EMT where despite the fact that repression E-Cad is a crucial step in this process (Cano et al., 2000; Batlle et al., 2000; reviewed in (Huber et al., 2005), overexpression of E-Cad alone is not sufficient to block EMT (Ohkubo and Ozawa, 2004).

Vertebrate GATA6 Induces a Similar EMT in MDCK Cells

Vertebrate orthologs of Srp, GATA 4, 5, and 6 (Gillis et al., 2008) are similarly expressed and implicated in the differentiation of various organs of endodermal origin such as intestine, colon, and liver (Gao et al., 1998; Molkentin, 2000). These genes appear to have distinct roles in mammalian development and pathogenesis. In particular, hGATA6 has recently been reported to be upregulated in some human cancers of endoderm origin (Shureiqi et al., 2007; Fu et al., 2008; Kwei et al., 2008), and an increased accumulation of hGATA6 has also been found in cells at the leading front of some endodermal tumors (Haveri et al., 2008).

To study the putative role of hGATA6 in EMT, we engineered MDCK cells to inducibly express hGATA6. This epithelial cell line has previously been instrumental in discovering the role of Snail, Slug, and Twist in EMT (Cano et al., 2000; Yang et al., 2004; Bolós et al., 2003). Expression of hGATA6 in MDCK cells caused a dramatic conversion toward a spindle mesenchymal-like phenotype as opposed to the epithelial morphology of non-induced control cells (Figures 6B and 6E). This morphological change was concomitant with a loss of membrane-associated E-Cad, which accumulated in punctae in the cell cytoplasm (Figures 6C and 6F), but does not change in overall protein levels (Figure 6I). hGATA6 also induced remodeling of F-Act from the cell cortex to stress fibers as well as to motile structures similar to lamellipodia (Figures 6C′ and 6F′). Furthermore, hGATA6-expressing cells displayed membranous N-Cadherin (N-Cad) (Figures 6G and 6H), a well-established marker gene of mesenchymal cell (Moreno-Bueno et al., 2009). To test for changes in migratory and invasive capacity in hGATA6 expressing cells, we performed assays on collagen type IV-coated Transwells. We found that hGATA6 expression greatly enhances the motility of MDCK cells, in comparison to noninduced control cells (Figures 6J–6L). Together these results show that hGATA6 triggers a loss of epithelial traits, acquisition of fibroblastic morphology and increases motility and invasive capacity in MDCK cells.

Srp and GATA6-Induced Transitions Share Some Features

To further explore the similarities between Srp and hGATA6-induced transitions, we next investigated for changes in the RNA levels of *e-cad* upon expression of hGATA6. We found that similar to Srp, hGATA6 does not repress *e-cad* transcription, as there are no significant differences in *e-cad* RNA levels between hGATA6-expressing MDCK cells and noninducible controls (Figure 6M). Thus, both Srp and hGATA6-induced transitions occur without abolishing *e-cad* transcription.

We next examined for changes in the RNA levels of members of the Crumbs complex upon expression of hGATA6. There are three vertebrate Crumbs genes—*crb1*, *crb2*, and *crb3*—and, of these, just *crb2* and *crb3* are expressed in MDCK cells (Roh and Margolis, 2003). We found that while *crb3* RNA expression levels do not change upon hGATA6 expression, *crb2*, is strongly downregulated (Figure 6M). Other members of the Crb complex, *protein associated with Lin-7 (pals1)* or *Pals1-associated tight junction protein (PATJ)*, did not show any changes at the RNA level (Figure 6M). Next, we made use of a published data set of hGATA6 binding sites that was generated from an hGATA6 RNA-seq experiment performed on the human intestinal Caco-2 cell line (Verzi et al., 2010). We searched their processed data for positive hGATA6 binding peaks in the regulatory regions of crb2 and crb3 and found that while there are no peaks in *crb3, crb2* has a positive GATA6-binding peak within its first intron (Verzi et al., 2010). Genomic alignment shows that the hGATA6 binding region is conserved from humans to dogs (data not shown), further supporting the idea that similar to Srp in flies, hGATA6 represses *crb2* in MDCK cells through direct binding to a regulatory region within the first intron of *crb2*.

Finally, we assayed for changes in the expression of Claudin genes, and found that *claudins 1*, *7*, and *16* are all strongly repressed by hGATA6 (Figure 6M), while expression of hGATA6 induces an upregulation of *mmp1* (Figure 6M). Thus, the repression of Claudin genes and activation of *mmp1* are also a conserved feature of Srp and hGATA6-induced transitions.

Vertebrate hGATA4 Also Induces an EMT in MDCK Cells

As mentioned above, other vertebrate GATA factors such as GATA4 and 5 are also closely related to Srp. Thus, we performed with hGATA4 and hGATA5 similar experiments in MDCK cells as those performed with hGATA6 and found that hGATA4 has a similar effect to hGATA6 (Figures S6G and S6H). However, EMT was not induced by hGATA5 (Figures S6E and S6F). This indicates the specificity of the transformation, which appears not to be a common feature of all GATA factors, and is in agreement with the observation than the vertebrate GATA4 and 6 are both more closely related to each other than to the GATA5 gene (Lowry and Atchley, 2000; Gillis et al., 2008). Furthermore, GATA4 and 6 have recently been reported to have overlapping functions in the regulation of proliferation and differentiation of intestinal cells (Beuling et al., 2011). As a control, we also induced the expression of a mutated form of hGATA6 (which contains point mutations in both zinc fingers and thus cannot bind to DNA) and found that it did not induce an EMT (Figures 6I and 6J). Although it is still not clear which are the mechanisms involved in hGATA6 induced E-Cad protein relocalization, altogether, these results demonstrate that among some GATA factors, the ability to induce a distinct EMT without silencing E-Cad transcription is a conserved feature from flies to humans.

DISCUSSION

In this study, we investigate the role of Srp in the *Drosophila* endoderm, and show that it is required to induce endoderm cells to switch from an epithelial to nonpolarized motile behavior, and that it acts as a potent trigger of a similar transition when misexpressed spatially or temporally in epithelial cells. Srp promotes dE-Cad junctional downregulation and while Srp is likely to impinge on a large number of genes, a specific feature of its activity is *crb* transcriptional repression. In addition, we have also shown that the overexpression of either hGATA6 or 4 in MDCK cells triggers a distinct EMT, which shows many similarities to the Srp-induced transition, as changes in cell polarity, adhesion, and motility occur without any changes in E-Cad at the RNA or protein levels, while a crb ortholog, *crb2* becomes strongly repressed.

Cells traditionally have been classified as epithelial or mesenchymal depending upon whether they are polarized or not, possess junctions or have lost adhesion, and display static or migratory and invasive behavior. Here, we show that during the formation of the endoderm, cells lose apico-basal polarity and become highly motile, a common feature of both developmental and pathological EMTs. However, a distinct feature of the endodermal transition is that while adherens junctions become fragmented, dynamic puntae of dE-Cad protein are maintained at the plasma membrane. Despite their highly mesenchymal appearance, endoderm cells migrate as a collective mass. Thus, spots of dE-Cad may be retained at the membrane during this type of transition to facilitate collective, rather than individual migration. It should be noted, this is very different to other types of collective migration, which have described for epithelial cells in the *Drosophila* embryo, such as in the trachea, where cells

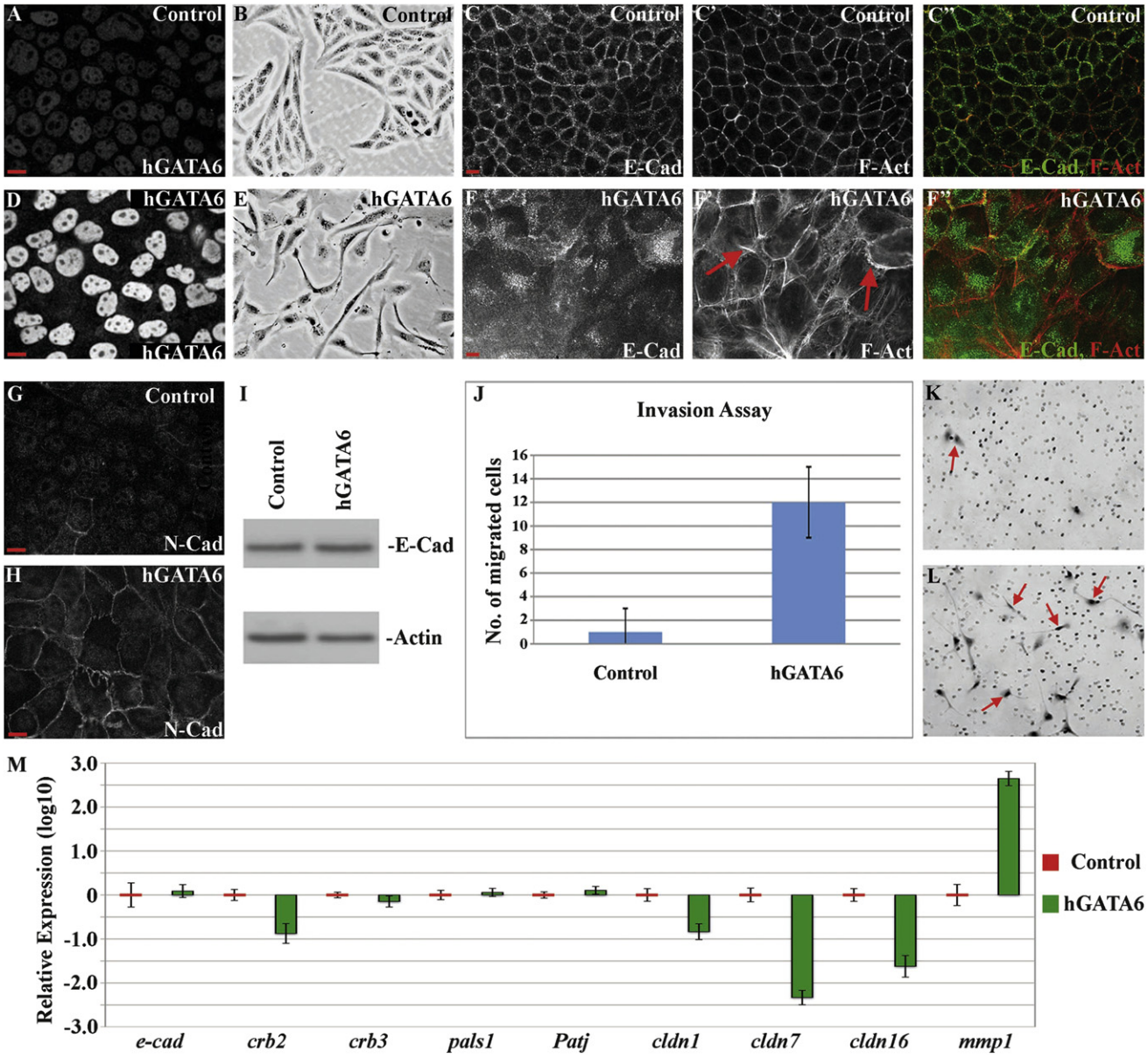

Figure 6. hGATA6 Induces EMT in MDCK Cells

(A–H) MDCK-hGATA6-dox cells before (A, B, C, and G) and 6 days after induction of hGATA6 expression (D–F and H). (A and D) Nuclear accumulation of hGata6 protein after addition of doxycycline. (B and E) hGATA6-induced MDCK cells adopt a mesenchymal-like spindle shaped morphology. (C and F) Single confocal slice of cells stained for F-Act and E-Cad. The normal junctional localization of E-Cad is lost, and instead E-Cad is found in punctate dots in the cell cytoplasm. F-Act appears reorganized into stress fibers and lamellipodia-like structures (F′, arrows). (G and H) N-Cad is found localized at the cell membrane of hGATA6-induced cells.

(I) Western blot analysis show that hGATA6 expression does not induce changes in the levels of E-Cad protein.

(J) The migratory and invasion capacity of control and hGATA6-induced MDCK cells was analyzed in transwell assays on matrigel 96 hr after hGata6 induction. hGATA6-induced cells possessed a 10-fold increase in migration/invasion behavior. Eight randomly selected microscopic fields (20× magnification) were imaged to calculate the average number of occupied pores per microscopic field. Results represent the mean ± SD of at least two independent experiments performed in duplicate.

(K and L) Cells migrated through the matrigel to the bottom (K and L, arrows). (M) qPCR analysis shows the relative expression changes, in log10 scale, of the indicated genes in hGATA6 expressing MDCK cells (green) compared with the noninduced controls (red) 48 hr after doxycycline induction. Gene expression levels were normalized using the endogenous control GAPDH.

Error bars indicate SD. Scale bars, 10 μm. See also Figure S6.

migrate, but do not lose apico-basal polarity or disassemble cell junctions.

EMT in the mesoderm and almost all EMTs studied to date have been shown to rely on the activity of *sna* genes (Barrallo-Gimeno and Nieto, 2005). The few other cases that do not depend on *sna* genes rely on the activation of other *e-cad* transcriptional repressors such as E47 (Thiery et al., 2009). In contrast, the transition reported here occurs independently of Sna and does not rely on E-Cad transcriptional repression. Thus, the endodermal-transition is distinct from canonical EMTs not only at the morphological, but also at the transcriptional level. One way of achieving different degrees of adhesion between cells subsequent to EMT could be to drive Sna at different levels; however, this could be more difficult to achieve and more prone to errors than activating an independent mechanism. Thus, rather than activating a single EMT mechanism at different intensities, Srp appears to be an alternative trigger for this distinct kind of EMT in which low levels of dE-Cad are retained at the membrane.

We and others have reported many cases where E-Cad is downregulated at the protein level during development (i.e., Shaye et al., 2008). This also occurs during EMT in gastrulating mouse embryos, where p38 downregulates E-Cad at the protein level by a mechanism independent of transcriptional repression by Sna (Zohn et al., 2006). However, what is different about the Srp-induced epithelial transition reported here, is that while it is also not linked to *dE-cad* gene repression, it is both necessary and sufficient to induce a transition to nonpolarized, motile cell behavior. This contrasts with other reported cases, such as in the *Drosophila* trachea, where dE-Cad is downregulated, but this is not sufficient to induce a loss of cell polarity. In the case of mouse gastrulation, *sna* mutant cells fail to undergo EMT (Carver et al., 2001; Barrallo-Gimeno and Nieto, 2005), indicating that the p38-dependent E-Cad delocalization is not sufficient to drive EMT and in p38 mutants there is still some EMT (Zohn et al., 2006), indicating that the p38 pathway is not absolutely required for EMT. This strongly contrasts with the Srp pathway, which is absolutely required and sufficient to drive a transition to nonpolarized migratory cell behavior.

The specific features of the Srp-induced EMT are likely to facilitate cohesive cell migration, and it seems easier to revert to epithelial again, a case often found both in development and tumor progression. Indeed, the collective invasion of cells that display combination of epithelial and mesenchymal features rather than a full conversion to a mesenchymal phenotype is prevalent in many cancer types (Friedl and Gilmour, 2009). The finding that GATA factors play a conserved role in inducing a similar epithelial transition in mammalian cells and that high levels of expression of hGATA6 are found in a number of endodermal tumors highlight the relevance of our results for development and cancer research. Further studies will be required to assess whether hGATA6 expression in such tumors induce similar changes in cell behavior to those seen in flies and MDCK cells.

EXPERIMENTAL PROCEDURES

Immunohistochemistry, In Situ Hybridization, Image Acquisition, and Analysis

Embryos were fixed, mounted, and staged using standard techniques. Embryos were stages according to the staging scheme in (Hartenstein, 1993). To determine exactly when EMT takes place in the PMG, embryos were collected over 30 min time periods, and then analyzed for markers for EMT. Antibodies and probes used are detailed in the Supplemental Experimental Procedures. Confocal images were acquired with a Leica SP5. Images were post-processed with Adobe Photoshop and ImageJ.

Chromatin Immunoprecipitation

Chromatin immunoprecipitation (ChIP) experiments were carried out as described previously (Sandmann et al., 2006). In each ChIP assay 4 independent chromatin samples were prepared from 0–6 hr wild-type embryo collections, two samples were incubated with anti-Srp sera and two samples without antibody, as a negative control. Each assay was preformed three times, and only regions that showed a strong enrichment in all three assays were considered to be positive for Srp binding. Primers used to assay for regions containing putative Srp-binding sites are listed in the Supplemental Experimental Procedures.

Quantification of RNA Levels in the PMG

The PMG was dissected from wild-type embryos at 3–3.5 hr (before), 6–6.5 hr (after), or from *srp* mutant embryos at 6–6.5 hr, according to the method described in (Skaer, 1989). Three PMGs were dissected per condition, RNA was isolated from the cells and amplified by Pico Profiling (Gonzalez-Roca et al., 2010). Four separate sample sets were isolated, and the RNA amounts quantified by quantitative real-time PCR. Primers used are detailed in the Supplemental Experimental Procedures. Gene expression levels were normalized using the endogenous control Actin5C for each sample, and differences in target gene expression were determined using the StepOne 2.2 software.

Immunofluorescence of MDCK Cells

MDCK cells were plated at a high confluence (150 000 cells/ml) and grown for 48 hr on sterile transparent 0.4 μm pore polyester membrane inserts (Corning 3470) coated with 2.5 $\mu g/cm^2$ laminin (Sigma, L2020). For full details of fixing and staining procedures, and antibodies used see Supplemental Experimental Procedures.

Invasion Assay

To obtain polarized monolayers for immunofluorescence, MDCK cells were seeded on transparent track-etched PET chambers, coated with matrigel. hGATA6 and control cells were seeded at a density of 5000 cells/well in DMEM medium supplemented with 0.5% BSA. Lower chambers were filled with 10% FBS to act as a chemoattractant. After 48 hr of incubation, the cells on the lower membrane surface were fixed and stained.

Quantitative Real-Time PCR on MDCK Cells

Total RNA samples were extracted using Trizol, DNAase treated, further purified using RNeasy columns (Qiagen), and reversed transcribed using the High Capacity cDNA Archive Kit (Applied Biosystems). RNA amounts were quantified by quantitative real-time PCR. Primers used are detailed in the Supplemental Experimental Procedures. Gene expression levels were normalized using the endogenous control GAPDH for each sample, and differences in target gene expression were determined using the StepOne 2.2 software.

SUPPLEMENTAL INFORMATION

Supplemental Information includes six figures, Supplemental Experimental Procedures, and six movies and can be found with this article online at doi:10.1016/j.devcel.2011.10.005.

ACKNOWLEDGMENTS

We are grateful to members of the Casanova and Llimargas labs and Angela Nieto and Montserrat Corominas for helpful discussions and to Nicolás Martín, Yolanda Rivera, and other members of ours and the Jiménez lab for technical assistance. We also acknowledge the Advanced Digital Microscopy, the Biostatistics/Bioinformatics Unit and the Functional Genomics Core Facilities from the Institute of Research in Biomedicine and the Bioinformatics Platform from the Consolider Project GESHAPE, CSD 2007-00008. We thank E. Furlong, D. Hoshizaki, E. Knust, J. Kumar, H. Oda, B. Sanson, S. Sotillos,

A. Wodarz, the Bloomington stock centre, and DSHB for kindly sending us flies and reagents. This work has been supported by the Generalitat de Catalunya, the Spanish Ministerio de Ciencia e Innovacion (MICINN) and its Consolider-Ingenio 2010 program to J.C., X.F.-M., and E.B. We also acknowledge support from the Programa Juan de la Cierva (K.C.) and the European Research Council (ERC-FP7) (E.B.).

Received: May 3, 2011
Revised: August 30, 2011
Accepted: October 6, 2011
Published online: December 12, 2011

REFERENCES

Barrallo-Gimeno, A., and Nieto, M.A. (2005). The Snail genes as inducers of cell movement and survival: implications in development and cancer. Development *132*, 3151–3161.

Batlle, E., Sancho, E., Francí, C., Domínguez, D., Monfar, M., Baulida, J., and García De Herreros, A. (2000). The transcription factor snail is a repressor of E-cadherin gene expression in epithelial tumour cells. Nat. Cell Biol. *2*, 84–89.

Beuling, E., Baffour-Awuah, N.Y., Stapleton, K.A., Aronson, B.E., Noah, T.K., Shroyer, N.F., Duncan, S.A., Fleet, J.C., and Krasinski, S.D. (2011). GATA factors regulate proliferation, differentiation, and gene expression in small intestine of mature mice. Gastroenterology *140*, 1219–1229, e1–e2.

Bolós, V., Peinado, H., Pérez-Moreno, M.A., Fraga, M.F., Esteller, M., and Cano, A. (2003). The transcription factor Slug represses E-cadherin expression and induces epithelial to mesenchymal transitions: a comparison with Snail and E47 repressors. J. Cell Sci. *116*, 499–511.

Campos-Ortega, J.A., and Hartenstein, V. (1985). The Embryonic Development of Drosophila melanogaster (Berlin: Springer-Verlag).

Cano, A., Pérez-Moreno, M.A., Rodrigo, I., Locascio, A., Blanco, M.J., del Barrio, M.G., Portillo, F., and Nieto, M.A. (2000). The transcription factor snail controls epithelial-mesenchymal transitions by repressing E-cadherin expression. Nat. Cell Biol. *2*, 76–83.

Cao, C., Liu, Y., and Lehmann, M. (2007). Fork head controls the timing and tissue selectivity of steroid-induced developmental cell death. J. Cell Biol. *176*, 843–852.

Carver, E.A., Jiang, R., Lan, Y., Oram, K.F., and Gridley, T. (2001). The mouse snail gene encodes a key regulator of the epithelial-mesenchymal transition. Mol. Cell. Biol. *21*, 8184–8188.

Friedl, P., and Gilmour, D. (2009). Collective cell migration in morphogenesis, regeneration and cancer. Nat. Rev. Mol. Cell Biol. *10*, 445–457.

Fu, B., Luo, M., Lakkur, S., Lucito, R., and Iacobuzio-Donahue, C.A. (2008). Frequent genomic copy number gain and overexpression of GATA-6 in pancreatic carcinoma. Cancer Biol. Ther. *7*, 1593–1601.

Gao, X., Sedgwick, T., Shi, Y.B., and Evans, T. (1998). Distinct functions are implicated for the GATA-4, -5, and -6 transcription factors in the regulation of intestine epithelial cell differentiation. Mol. Cell. Biol. *18*, 2901–2911.

Gillis, W.Q., Bowerman, B.A., and Schneider, S.Q. (2008). The evolution of protostome GATA factors: molecular phylogenetics, synteny, and intron/exon structure reveal orthologous relationships. BMC Evol. Biol. *8*, 112.

Gonzalez-Roca, E., Garcia-Albéniz, X., Rodriguez-Mulero, S., Gomis, R.R., Kornacker, K., and Auer, H. (2010). Accurate expression profiling of very small cell populations. PLoS ONE *5*, e14418.

Grawe, F., Wodarz, A., Lee, B., Knust, E., and Skaer, H. (1996). The Drosophila genes crumbs and stardust are involved in the biogenesis of adherens junctions. Development *122*, 951–959.

Hartenstein, V. (1993). Atlas of Drosophila Development (Cold Spring Harbor, NY: Cold Spring Harbor Laboratory Press).

Haveri, H., Westerholm-Ormio, M., Lindfors, K., Mäki, M., Savilahti, E., Andersson, L.C., and Heikinheimo, M. (2008). Transcription factors GATA-4 and GATA-6 in normal and neoplastic human gastrointestinal mucosa. BMC Gastroenterol. *8*, 9.

Hay, E.D. (1995). An overview of epithelio-mesenchymal transformation. Acta Anat. (Basel) *154*, 8–20.

Huber, M.A., Kraut, N., and Beug, H. (2005). Molecular requirements for epithelial-mesenchymal transition during tumor progression. Curr. Opin. Cell Biol. *17*, 548–558.

Kwei, K.A., Bashyam, M.D., Kao, J., Ratheesh, R., Reddy, E.C., Kim, Y.H., Montgomery, K., Giacomini, C.P., Choi, Y.L., Chatterjee, S., et al. (2008). Genomic profiling identifies GATA6 as a candidate oncogene amplified in pancreatobiliary cancer. PLoS Genet. *4*, e1000081.

Lowry, J.A., and Atchley, W.R. (2000). Molecular evolution of the GATA family of transcription factors: conservation within the DNA-binding domain. J. Mol. Evol. *50*, 103–115.

Molkentin, J.D. (2000). The zinc finger-containing transcription factors GATA-4, -5, and -6. Ubiquitously expressed regulators of tissue-specific gene expression. J. Biol. Chem. *275*, 38949–38952.

Moreno-Bueno, G., Peinado, H., Molina, P., Olmeda, D., Cubillo, E., Santos, V., Palacios, J., Portillo, F., and Cano, A. (2009). The morphological and molecular features of the epithelial-to-mesenchymal transition. Nat. Protoc. *4*, 1591–1613.

Myat, M.M., and Andrew, D.J. (2000). Fork head prevents apoptosis and promotes cell shape change during formation of the Drosophila salivary glands. Development *127*, 4217–4226.

Ohkubo, T., and Ozawa, M. (2004). The transcription factor Snail downregulates the tight junction components independently of E-cadherin downregulation. J. Cell Sci. *117*, 1675–1685.

Peinado, H., Olmeda, D., and Cano, A. (2007). Snail, Zeb and bHLH factors in tumour progression: an alliance against the epithelial phenotype? Nat. Rev. Cancer *7*, 415–428.

Reuter, R. (1994). The gene serpent has homeotic properties and specifies endoderm versus ectoderm within the Drosophila gut. Development *120*, 1123–1135.

Reuter, R., and Leptin, M. (1994). Interacting functions of snail, twist and huckebein during the early development of germ layers in Drosophila. Development *120*, 1137–1150.

Reuter, R., Grunewald, B., and Leptin, M. (1993). A role for the mesoderm in endodermal migration and morphogenesis in Drosophila. Development *119*, 1135–1145.

Revenu, C., and Gilmour, D. (2009). EMT 2.0: shaping epithelia through collective migration. Curr. Opin. Genet. Dev. *19*, 338–342.

Roh, M.H., and Margolis, B. (2003). Composition and function of PDZ protein complexes during cell polarization. Am. J. Physiol. Renal Physiol. *285*, F377–F387.

Sandmann, T., Jakobsen, J.S., and Furlong, E.E. (2006). ChIP-on-chip protocol for genome-wide analysis of transcription factor binding in Drosophila melanogaster embryos. Nat. Protoc. *1*, 2839–2855.

Sandmann, T., Girardot, C., Brehme, M., Tongprasit, W., Stolc, V., and Furlong, E.E. (2007). A core transcriptional network for early mesoderm development in Drosophila melanogaster. Genes Dev. *21*, 436–449.

Shaye, D.D., Casanova, J., and Llimargas, M. (2008). Modulation of intracellular trafficking regulates cell intercalation in the Drosophila trachea. Nat. Cell Biol. *10*, 964–970.

Shook, D., and Keller, R. (2003). Mechanisms, mechanics and function of epithelial-mesenchymal transitions in early development. Mech. Dev. *120*, 1351–1383.

Shureiqi, I., Zuo, X., Broaddus, R., Wu, Y., Guan, B., Morris, J.S., and Lippman, S.M. (2007). The transcription factor GATA-6 is overexpressed in vivo and contributes to silencing 15-LOX-1 in vitro in human colon cancer. FASEB J. *21*, 743–753.

Skaer, H. (1989). Cell division in Malpighian tubule development in D. melanogaster is regulated by a single tip cell. Nature *342*, 566–569.

Skaer, H. (1993). The alimentary canal. In Developmental Biology of Drosophila melanogaster, M. Bate and A. Martinez-Ariaz, eds. (Plainview, NY: Cold Spring Harbor Lab), pp. 941–1012.

Srivastava, A., Pastor-Pareja, J.C., Igaki, T., Pagliarini, R., and Xu, T. (2007). Basement membrane remodeling is essential for Drosophila disc eversion and tumor invasion. Proc. Natl. Acad. Sci. USA *104*, 2721–2726.

Tepass, U., and Hartenstein, V. (1994a). Epithelium formation in the Drosophila midgut depends on the interaction of endoderm and mesoderm. Development *120*, 579–590.

Tepass, U., and Hartenstein, V. (1994b). The development of cellular junctions in the Drosophila embryo. Dev. Biol. *161*, 563–596.

Tepass, U., Theres, C., and Knust, E. (1990). crumbs encodes an EGF-like protein expressed on apical membranes of Drosophila epithelial cells and required for organization of epithelia. Cell *61*, 787–799.

Tepass, U., Fessler, L.I., Aziz, A., and Hartenstein, V. (1994). Embryonic origin of hemocytes and their relationship to cell death in Drosophila. Development *120*, 1829–1837.

Tepass, U., Gruszynski-DeFeo, E., Haag, T.A., Omatyar, L., Török, T., and Hartenstein, V. (1996). shotgun encodes Drosophila E-cadherin and is preferentially required during cell rearrangement in the neurectoderm and other morphogenetically active epithelia. Genes Dev. *10*, 672–685.

Thiery, J.P., Acloque, H., Huang, R.Y., and Nieto, M.A. (2009). Epithelial-mesenchymal transitions in development and disease. Cell *139*, 871–890.

Uemura, T., Oda, H., Kraut, R., Hayashi, S., Kotaoka, Y., and Takeichi, M. (1996). Zygotic Drosophila E-cadherin expression is required for processes of dynamic epithelial cell rearrangement in the Drosophila embryo. Genes Dev. *10*, 659–671.

Verzi, M.P., Shin, H., He, H.H., Sulahian, R., Meyer, C.A., Montgomery, R.K., Fleet, J.C., Brown, M., Liu, X.S., and Shivdasani, R.A. (2010). Differentiation-specific histone modifications reveal dynamic chromatin interactions and partners for the intestinal transcription factor CDX2. Dev. Cell *19*, 713–726.

Yang, J., Mani, S.A., Donaher, J.L., Ramaswamy, S., Itzykson, R.A., Come, C., Savagner, P., Gitelman, I., Richardson, A., and Weinberg, R.A. (2004). Twist, a master regulator of morphogenesis, plays an essential role in tumor metastasis. Cell *117*, 927–939.

Yip, M.L., Lamka, M.L., and Lipshitz, H.D. (1997). Control of germ-band retraction in Drosophila by the zinc-finger protein HINDSIGHT. Development *124*, 2129–2141.

Zohn, I.E., Li, Y., Skolnik, E.Y., Anderson, K.V., Han, J., and Niswander, L. (2006). p38 and a p38-interacting protein are critical for downregulation of E-cadherin during mouse gastrulation. Cell *125*, 957–969.